ME-NETT23 The 23rd Conference of the Mechanical Engineering Network of Thailand

AMM-005465

The 23rd Conference of the Mechanical Engineering Network of Thailand
November 4 – 7, 2009, Chiang Mai

Modelling a Swaging Process of HDD Head Stack Assemblies

Chaloemsri K[1], and Bureerat S[1,*]

[1] Department of Mechanical Engineering, Khon Kaen University, Khon Kaen, Thailand 40002

*Corresponding Author: sujbur@kku.ac.th, Tel. 043-202845

Abstract

This paper presents a finite element model for simulating a swaging process of a hard disk drive (HDD) head stack assembly (HSA). A swaging process is a material processing technique used to connect a suspension system to an E-block becoming the so-called head stack assembly by using swage balls. The finite element (FE) model is 3-dimensional where solid Lagrangian elements and the explicit dynamics simulation are being used. In this paper, the base plate and arm tip deformation due to ball swaging are evaluated. The NHK base plate model is selected for FE simulation. The simulation results are compared to those obtained from experimentation. It was found that the results from FE analysis agree well with the experiment results.

Keywords*:* Finite element analysis, Swaging process, Hard disk drive, Contact analysis, Head stack Assembly.

1. Introduction

In the HDD manufacturing process, ball swaging is one of most important manufacturing processes, which joints the head gimbal assembly (HGA) base plates together with an actuator arm leading to the new part called a head stack assembly (HSA). The HGA base plate is a thin sheet component, which includes boss tower as illustrated in Figure 1. The boss tower is sized to fit within an opening in the actuator arm to which the HGA base plates to be mounted. During the swaging process, the ball is driven pass through the boss tower into frictional engagement with the inner surface of the opening in the actuator arm and clamped by swage keys. The baseplate and attached suspension are thereby securely fastened to the actuator arm. To hold the HGA in place, the interface between the base plate and actuator arm must develop a suitable minimum retention torque value. A specific value of retention torque at the joint is demanded to withstand the vibrations of the actuator arm that was induced by high-speed unstable airflow in the drive. A view of the assembly of swaging process is shown in Figure 2.

Unfortunately, the swaging process can result in plastic deformation of HGA base plate and actuator arm. This deformation can cause changes in a desired spring characteristics of the suspension on the actuator arm, known as gramload change from its nominal value, and change of desired retention torque. Since gram load and retention torque are the critical parameters affecting the slider flight height and op-shock performance of hard disk drives, investigating the swaging process induced base plate and arm deformation, gramload as well as retention torque change are of general interest.

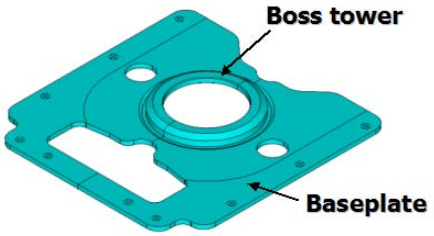

Fig.1 Components of a baseplate

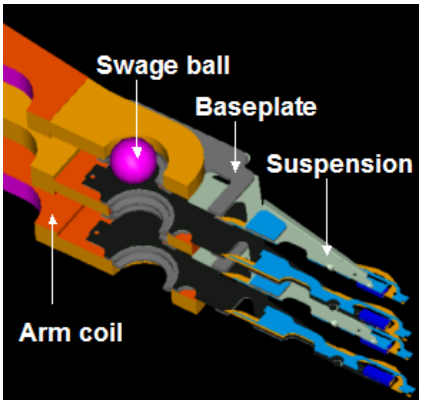

Fig. 2 The assembly for swaging process

The work by Wadhwa [1] is the one of the early analyses of the ball swaging process numerically using an axis-symmetric model of the in-plane deformation. Aoki and Aruga [2] performed an elasto-plastic large deformation analysis based on a symmetrical model for ball swaging and clarified that the baseplate is influenced by the arm deformation due to the asymmetric stress. Kamnerdtong et al. [3] numerically verified the effects of swaging process parameters including the size, velocity and shooting direction of the swage ball by using an axis-symmetric finite element analysis (FEA). Some of the recommendations had also been given regarding the torque resistance was dominated by contact pressure of the swaging process and unpleasant higher stress intensity in the necking zone of the baseplate resulting in higher deformation of the arm. Jian Yang et al. [4] performed a comprehensive three -dimensional finite element analysis of ball swaging process with 2 swage keys and 2-swage balls for both inner and outer arms with attached base plate(s). The changed of gram load on sliders is estimated from the nominal gram load value and gram load deviation due to the base plate and arm deformation. The estimated gram load values also correlate well with the average test data. Further work towards a swaging process and computational contact mechanics can be found in [5-9]. However, review of literature shows that investigating the swaging with bi-directional swaging by using 3-Balls induced gram load and retention torque change are still open and challenging.

The aim of this work is to determine the effects from bi-directional swaging process by initiating comprehensive three dimensional finite element analysis model (FEA). In the present work, the swaging process is studied by performing explicit dynamic finite element analysis (FEA) using a commercial program ANSYS/LS-

Dyna. Both one-sided and two-sides top arm in the assembly are opted as a prototype to be studied. 3-Balls swaging process is considered where the ball diameters are 0.0780"(1st pass), 0.0810"(2nd pass), 0.0820" (3rd pass flip), and its velocity maintains constant at 0.7in/s in the top-to-bottom direction.

2. Finite Element Modeling

The use of finite element analysis for material processing techniques, particularly for those involving contact mechanics, has been studied for many years [9]. A contact system of multiple deformable bodies can be thought of as the system being in an equilibrium state such that contact constraints (no penetration between bodies) are imposed on the surfaces of the bodies touching each other. The equation of motion of a body occupying a space domain Ω can be written as [9]

$$\frac{\partial \sigma_{ji}(\mathbf{x},t)}{\partial x_j} + b_i(\mathbf{x},t) = \rho a_i(\mathbf{x},t) \quad \text{for } i = 1, \ldots, 3 \text{ and } j = 1, \ldots, 3 \tag{1}$$

Where **x** is a point on Ω, σ_{ji} is a Cauchy stress component, **b** is a body force vector, ρ is material density, and **a** is an acceleration vector. The boundary of the body Ω can be defined as Γ, and it is divided into three distinct parts as

$$\Gamma = \Gamma_d \cup \Gamma_f \cup \Gamma_c \tag{2}$$

where Γ_d is the boundary part having prescribed displacements, Γ_f is the boundary part that has prescribed forces, and Γ_c the boundary part contacting to other bodies. The prescribed boundary conditions can be written as

$$\begin{aligned} u_i(\mathbf{x},t) &= \bar{u}_i(\mathbf{x},t); \mathbf{x} \in \Gamma_d \\ \sigma_{ij}(\mathbf{x},t) N_j &= \bar{q}_i(\mathbf{x},t); \mathbf{x} \in \Gamma_f \end{aligned} \tag{3}$$

Where $\bar{u}_i$ and $\bar{q}_i$ are prescribed displacement and boundary traction components respectively. N_j is the component of an outward normal vector at **x** on Γ_f. The initial conditions for displacement (**u**) and velocity (**v**) are also required as:

$$\begin{aligned} \mathbf{u}(\mathbf{x},0) &= \bar{\mathbf{u}}(\mathbf{x}); \mathbf{x} \in \Omega \\ \mathbf{v}(\mathbf{x},0) &= \bar{\mathbf{v}}(\mathbf{x}); \mathbf{x} \in \Omega \end{aligned} \tag{4}$$

Where $\bar{\mathbf{u}}$ and $\bar{\mathbf{v}}$ are prescribed displacement and velocity respectively. The contact constraints are assigned in such a way that the contact stress should be negative (or compressive) whereas there is no penetration between bodies. The contact constraints on Γ_f can be expressed as:

$$\begin{aligned} g(\mathbf{x},t) &= g(\mathbf{x},0) - \mathbf{u}(\mathbf{x},t) \cdot \mathbf{N} \geq 0; \mathbf{x} \in \Gamma_c \\ \bar{\mathbf{q}}_c(x,t) \cdot \mathbf{N} &\leq 0; \mathbf{x} \in \Gamma_c \end{aligned} \tag{5}$$

Where g is the gap between contact surfaces, and $\mathbf{q}_c$ is the contact traction.

By means of finite element analysis, the mathematical model (1) to (5) can be simplified to the matrix from of the system of second order differential equations. The system of differential equations can then be solved by using implicit and explicit time integration techniques. Several numerical schemes dealing with the contact constraints (5) have been proposed such as the

Lagrange multiplier method, the augment Lagrangian method, and the penalty method. The methods have been implemented on numerous real world contact problems successfully.

3. Swaging Process Modeling

The finite element simulation of the ball swaging process was performed with the commercial software package. A three-dimension (3-D) view and a cross-sectional view of the finite element (FE) model used for swaging process of actuator arms are shown in Figure 3.

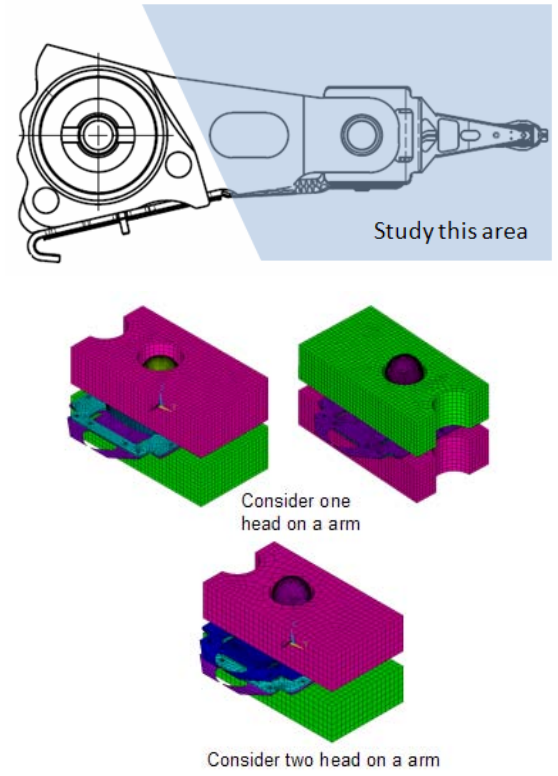

Fig. 3 3-D view of the finite element model used for swaging simulation of an actuator arm and attached base plates

In this simulation, we performed a nonlinear explicit dynamics analysis. If the stress is in the elastic deformation region, the relationship between stress and strain is linear. After the stress reaches the yield point, the relationship becomes nonlinear. The swaged part of the base plate undergoes plastic deformation. Nonlinear material properties should be considered. Geometric nonlinearity is also considered in this analysis because the base plate undergoes large deformation at the swaged part, as shown in Figure 4.

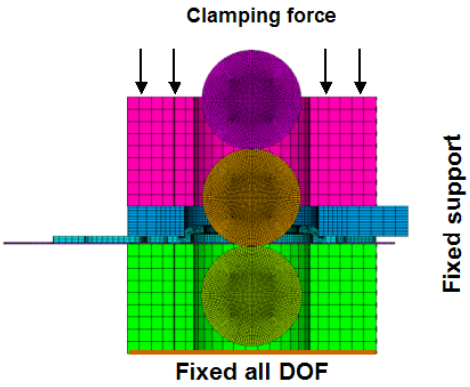

Fig. 4 Boundary conditions of the FE model cross section

The model includes an actuator arm tip, two base plates with part of hinges, two swage keys, and three swage balls. The model was separated to two types of assembly for analyze, the base plate attached one-side and two-sides as shown in Figures 5. The NHK base plate model illustrated in Figure 6 is chosen to investigate. To incorporate the elastic-plastic behavior of the actuator arm and base plates, these parts are modeled as bilinear isotropic material for baseplate and hinge, and bilinear kinematics hardening materials of an aluminum actuator arm.

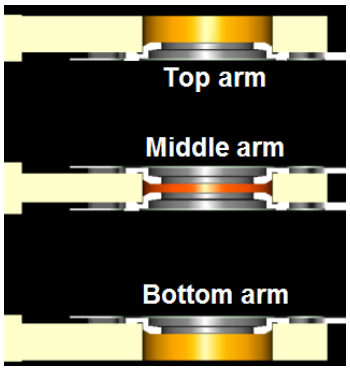

Fig.5 model for one-sided and two-sided swaging

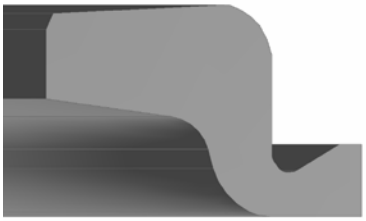

Fig. 6 NHK base plate model

3.1 Boundary Conditions and Contact Surfaces

During the swaging process, the constant clamping force at the outer parts during swaging is 65 psi and the arms are separated from each other by the use of spacer keys. In the FE model, the clamping pressure is applied as forces acting at a reference point on a prepared area. For simplicity, the swage keys, which are employed to simulate the clamping boundary at the arm contact condition, are modeled as rigid bodies while the other components including actuator arm tip, base plates and hinges are deformable parts. The simulation use the same load curve for ball speed for each heads and swage ball is forced to move in *Z* direction only.

The boss of the base plate is plastically deformed and joined to the arm. The contact surface between the ball and swaging boss, between the base plate and the arm, and the one between swaging boss and the clamp are taken into account in analyzing the contact pressure. The friction coefficients for each contact surface are separated as 2 groups, contact surface of assembly and part-to-part.

3.2 Material Properties

The base plate, hinge and the suspension are made of stainless steel while the arm is made of aluminum. The swaging ball is made of stainless steel with hardened coating. Thus, the ball is simulated as a rigid body. The material models defined in the analysis are bilinear isotropic material and bi-linear kinematics hardening. The properties of the materials used in the simulation are listed in Table 1.

Table 1 Material properties for finite element analysis

Material Properties	Type of Material	
	Stainless steel	Aluminum
Elastic modulus, E (MPa)	190,000	71,016
Yield stress, Y (MPa)	206	275
Poisson ratio	0.32	0.33
Mass density (kg/m^3)	7889	2700

All the elements used in the analysis are eight-nodes brick elements. To reduce the computing time, the model consists of both rigid bodies and deformable bodies. The actuator arm hole and the base plate boss tower are prepared such that finer meshes are only required in the vicinity of the contact areas and the elements are

coarser in the areas farther away. Meshing of the structure is portrayed in Figure 7.

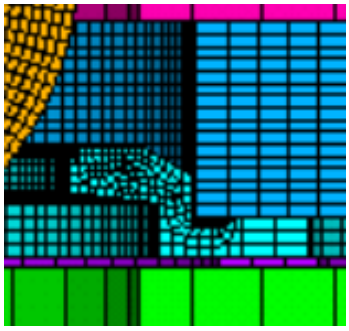

Fig. 7 Meshing of the cross section finite element model

3.3 Loading Conditions and Analysis

The analysis is performed through the following steps. Firstly, a compressive clamping force is applied to the prepared area on top of the spacer key. Next, the swaging ball is driven through. After the swage ball passing through, the clamping force is then released. After that, the upper and lower keys are ejected to allow final deformation of the assembly. The results for tip height, tip pitch and the reaction force at the ball are evaluated. The deformation is measured and evaluated on each node. The node location and section for measurement are determined.

4 Validation of the Finite Element Model

The base plate and arm tip deformation results from FEA simulations for inner and outer arms are evaluated from the displacements value that measured from specific nodes compared to the reference plane. The measurement section is shown in Figure 8. Then, the results are calculated and reported as Tip Height and Tip pitch deviation from nominal value, which is multiplied by a correction factor. For all simulated cases, the simulation results are intendancy to value from experimentation. However, there is some offset that required further investigation. These differences could be from some other effects not considered in the present analysis, such as the uncertainties of swage key shape and swage boss profile which different from actual parts. The illustrates of baseplate deformation from swaging process are shown in Fig.9

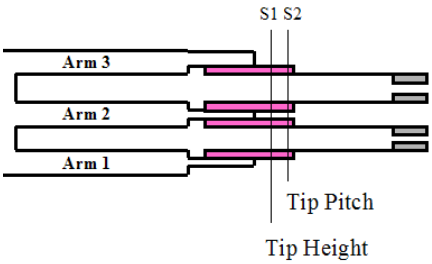

Fig. 8 Measurement point for arm Tip Height and Tip pitch

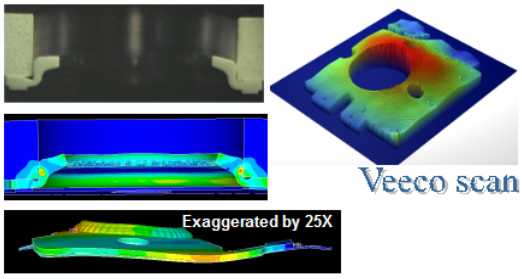

(a)

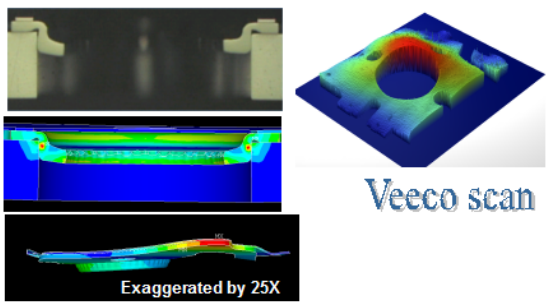

(b)

Fig. 9 FEA results of baseplate deformation from swaging process (exaggerated by 25 times) for (a) DN facing head and (b) UP facing head

Table 2 shows the comparison the tip height and tip pitch obtained from FE simulation and experiment. It can be seen that the computational results acceptably agree with that from experimantation. Thus, this finite element model will be used for gramload calculation in the future work.

Table 2 Simulation and experimental results

Parameters		Tip Height (inch)		Tip Pitch (degree)	
		FEA result	Actual data	FEA result	Actual data
Head 0	Outer arm	0.00153	0.00123	-0.737	-0.535
Head 1	Inner arm	-0.00146	-0.00192	-0.469	-0.320
Head 2	Inner arm	-0.00050	-0.00060	-0.233	-0.216
Head 3	Outer arm	0.00064	0.00070	0.581	0.347

4.1 Gram Load Calculation

The definition of gram load is the reaction force at the load point when the suspension assembly is elevated to offset height. The gram load on sliders also can be estimated by using Tip height and Tip Pitch from FE simulation. The gram load will be calculated from a specific equation at the effective slider z-height at loaded state.

5. Results and Discussions

The present work studies the behaviors and characteristics of the baseplate after a swaging process. The effects of changing the base plate and arm tip deformation to tip height and tip pitch deviation from nominal value are also investigated. Based on the result of this work, an offset could be diminished by improving the precision of swage key shape and swage boss profile. The result from this simulation will be used for evaluation of gram load and retention torque data. For this preliminary study, the FE simulation results are said to agree well with the actual experiment. The effects of ball swaging process on the resulting gram load and retention torque of HGA will be evaluated in future simulation.

6. Acknowledgment

This study is supported by Cooperate Project between National Electronics and Computer Technology Center (NECTEC) and Seagate Technology (Thailand) via Industry/University Cooperative Research Center (I/UCRC) in HDD Component, Khon Kaen University.

7. References

[1] S. K. Wadhwa, “Material Compatibility and Some Understanding of the Ball Swaging Process,” IEEE Trans. Magn., vol. 32, no. 3, pp. 1837-1842, May 1996

[2] K. Aoki and K. Aruga, “Numerical Ball Swaging Analysis of Head Arm for Hard Disk

Drives," Microsyst. Technol., vol. 13, pp. 943-949, 2007.

[3] T. Kamnerdtong, S. Chutima and K. Ekintumas, "Effects of Swaging Process Parameters on Specimen Deformation," Eighth Asian Symposium on Visualization, Chiangmai, Thailand, 2005, pp.50.1-50.7.

[4] Jian Yang, Chen-Chi Lin, Shahab Tabrizi, "Finite Element Simulation of Ball Swaging Process of Jointing HGA With Actuator Arm and Gram Load Calculation", ASME Information Storage and Processing Systems Conference, Santa Clara, CA, 2007

[5] Jongpradist, P.., Rotbunsongsri, R., Sukkana, C., Sungtong, W. Parametric Study of Baseplate Geometry Using Finite Element Analysis, DST-CON 2009, Bangkok, Thailand

[6] J.R. Cho, J.I. Song, K.T. Noh and D.H. Jeon, Nonlinear finite element analysis of swaging process for automobile power steering hose, Journal of Materials Processing Technology, Volume 170, Issues 1-2 , 14 December 2005, Pages 50-57

[7] Drean M.; Habraken A.M.; Muzeau J.P.; Bouchair A., Modelling of the Swaging Process during the Installation of Swaged Bolts, Journal of Constructional Steel Research, Volume 46, Number 1, April 1998, pp. 256-257(2)

[8] Li RONG, Zuo-ren NIE and Tie-yong ZUO, FEA modeling of effect of axial feeding velocity on strain field of rotary swaging process of pure magnesium, Transactions of Nonferrous Metals Society of China, Volume 16, Issue 5, October 2006, Pages 1015-1020

[9] Zhi-Hua Zhong, Finite element procedures for contact-impact problems, Oxford science publication, Oxford, 1993